Cyclic AMP regulates the HERG K+ channel by dual pathways

Jie Cui*, Yonathan Melman*, Eugen Palma*, Glenn I. Fishman† and Thomas V. McDonald*

Lethal cardiac arrhythmias are a hallmark of the hereditary Long QT syndrome (LQTS), a disease produced by mutations of cardiac ion channels [1]. Often these arrhythmias are stress-induced, suggesting a relationship between β-adrenergic activation of adenylate cyclase and cAMP-dependent alteration of one or more of the ion channels involved in LQTS. Second messengers modulate ion channel activity either by direct interaction or through intermediary kinases and phosphatases. Here we show that the second messenger cAMP regulates the K+ channel mutated in the LQT2 form of LQTS, HERG [2], both directly and indirectly. Activation of cAMP-dependent protein kinase (PKA) causes phosphorylation of HERG accompanied by a rapid reduction in current amplitude, acceleration of voltage-dependent deactivation, and depolarizing shift in voltage-dependent activation. In a parallel pathway, cAMP directly binds to the HERG protein with the opposing effect of a hyperpolarizing shift in voltage-dependent activation. The summation of cAMP-mediated effects is a net diminution of the effective current, but when HERG is complexed with with the K+ channel accessory proteins MiRP1 or minK, the stimulatory effects of cAMP are favored. These findings provide a direct link between stress and arrhythmia by a unique mechanism where a single second messenger exerts complex regulation of an ion channel via two distinct pathways.

Addresses: *Section of Molecular Cardiology, Departments of Medicine and Molecular Pharmacology, Albert Einstein College of Medicine, Bronx, New York, New York 10461, USA. †Section of Myocardial Biology, Zena and Michael A. Wiener Cardiovascular Institute, Departments of Medicine, Physiology & Biophysics and Biochemistry and Molecular Biology, Mount Sinai School of Medicine, One Gustave L. Levy Place, New York, New York 10029, USA.

Correspondence: Thomas V. McDonald
E-mail: mcdonald@aecom.yu.edu

Received: **1 December 1999**
Revised: **28 February 2000**
Accepted: **3 April 2000**

Published: **19 May 2000**

Current Biology 2000, 10:671–674

0960-9822/00/$ – see front matter

Results and discussion

Although the rapidly activating delayed rectifier (I_{Kr}) and it pore-forming subunit HERG have been thought to be insensitive to cAMP-dependent regulation [2,3], recent reports have shown PKA-mediated effects on HERG [4,5]. Moreover, sequence homology of the carboxyl terminus of HERG with cyclic nucleotide binding proteins suggests that cAMP might regulate I_{Kr} independent of its activation of PKA. Thus, we examined the effects of cAMP on HERG K+ channels in a heterologous mammalian expression system. Voltage-activated potassium currents typical of HERG/I_{Kr} were measured in CHO cells expressing cloned HERG under whole-cell patch clamp before and after addition of the membrane-permeable cAMP analog, 8-chlorophenylthio-adenosine 3:5′-cyclic monophosphate (CPT-cAMP). A consistent decrease in K+ current amplitude occurred within 3 minutes after introduction of 500 μM CPT-cAMP (Figure 1a,c). With the current reduction, we observed acceleration in the kinetics of voltage-dependent deactivation. Both effects occurred within the first 3 minutes of CPT-cAMP administration and persisted for the duration of the experiments. CPT-cAMP reduced HERG current by about 40% at all potentials (Figure 1b). Both the fast and slow time constants of deactivation were accelerated with the greatest effects at more positive potentials (Figure 1d). The relative contribution of the fast time constant was increased at all potentials (Figure 1d, inset). When the data were independently normalized to unity before and after cAMP, no significant change in voltage-dependence of activation or inactivation due to cAMP was seen (Figure 1b, insets). Voltage curves were fitted by a Boltzman function, $I = 1/(1 + exp[(V_h - V)/k])$, where I is the relative tail current amplitude, V is the test potential, V_h is the test potential producing half-maximal current, and k is the slope factor. Analysis revealed a small depolarizing shift in activation after cAMP addition (V_h(baseline) = –5.1 ± 0.18 mV, k = 11.1 V_h(cAMP) = –4.0 ± 0.26 mV, k = 11.1). cAMP therefore decreases effective HERG activity through current inhibition and accelerated deactivation kinetics with minimal alteration of voltage-dependent activation.

To assess whether cAMP was acting on HERG through PKA, the specific peptide inhibitor PKI was included in the patch pipette and cells were studied after pre-incubation with membrane-permeable myristolated PKI. PKI abolished the cAMP-mediated changes in deactivation kinetics and prevented nearly all of the cAMP-mediated current reduction (Figure 2a). While cAMP alone caused a modest positive shift in voltage-dependence of activation in HERG (+1.1 mV), in the presence of PKI, cAMP produced a leftward shift in both current–voltage and activation curves of 7.5 ± 0.3 mV

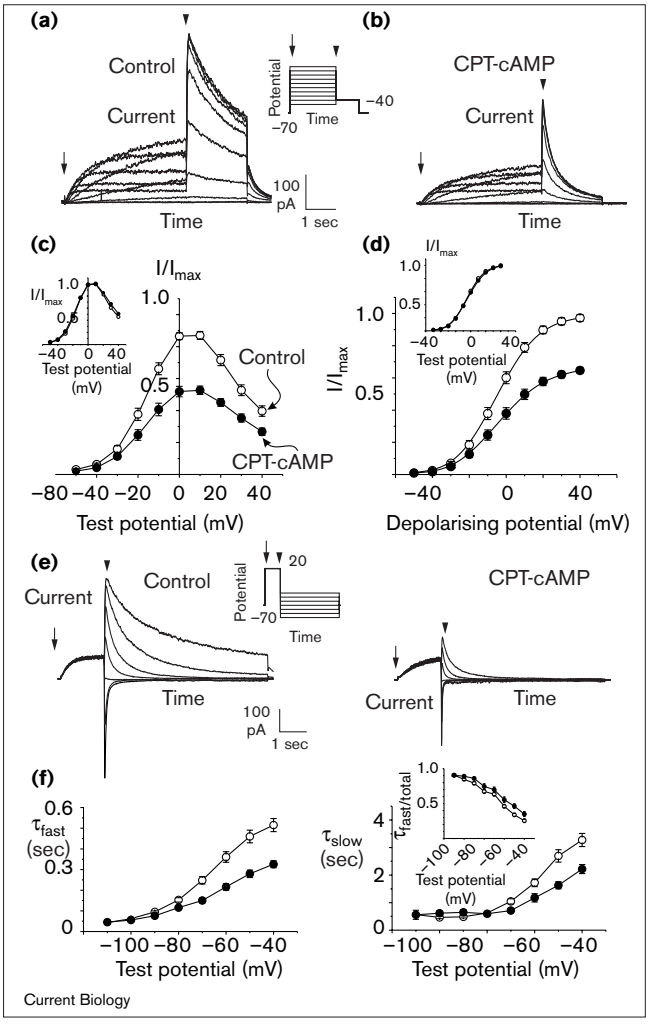

Figure 1

cAMP-mediated effects on HERG K^+ currents expressed in CHO cells. **(a,b)** Current tracings (a) before and (b) 3 min after treatment with 500 μM CPT-cAMP. Currents were elicited by 4 sec depolarizing steps to various levels followed by a repolarizing step to −40 mV (starting at arrowheads). Scale bars, 100 pA and 1 sec. **(c)** Current–voltage (I–V) relation curve (relative current amplitude, I/I_{max}, during depolarizing steps plotted against the step potential, I_{max} = maximal current before cAMP) before and after CPT-cAMP (means ± SEM $n = 42$). Inset, data were normalized to unity before and after cAMP, showing that there is no shift in the current–voltage relation. **(d)** Voltage-dependent activation curves plotted from peak tail currents during a repolarizing step to −40 mV after depolarizing to various voltages as in (a). Inset, the same data normalized to the maximum current in the same curve. **(e)** Repolarizing tail currents before and after treatment with CPT-cAMP, showing current reduction and acceleration of deactivation. Voltage clamp protocol, as shown in the central diagram: holding potential −70 mV, depolarizing step to 20 mV for 1.7 sec (arrows), repolarizing steps for 6 sec (arrowheads). **(f)** Summary of deactivation kinetic analysis shows acceleration of both fast (left graph) and slow (right graph) time constants of deactivation in a voltage dependent fashion. Inset, relative contribution of fast time constant vs. voltage. White circles, control; black circles, after treatment with CPT-cAMP.

negative from baseline ($V_{\frac{1}{2}}$(baseline) = –3.1 ± 0.22 mV, k = 10.8 $V_{\frac{1}{2}}$(cAMP) = –11.6 ± 0.37 mV, k = 12.0). PKI also prevented the cAMP-dependent acceleration of deactivation previously seen (data not shown). No significant changes in current density or deactivation kinetics were elicited by cGMP (data not shown), confirming the cAMP-specificity of our observed effects.

We identified four potential consensus sequence sites for phosphorylation by PKA, (Ser280, Ser887, Thr892, and Ser1134), all predicted to be at intracellular locations. We mutagenized these amino acids to alanines in various combinations to produce a panel of non-PKA phosphorylatable mutants (Figure 3a). Immunoprecipitation of HERG via a carboxy-terminal Myc epitope tag revealed that the channel protein could be ^{32}P-phosphorylated *in vivo* in a cAMP-dependent fashion (Figure 3b). HERG protein could also be phosphorylated *in vitro* with the purified catalytic subunit of PKA and [γ-^{32}P]ATP (Figure 3c). In contrast to the wild-type channel protein, HERGΔP1–4, a mutant with all four PKA sites removed, was not ^{32}P-phosphorylated in a cAMP-dependent manner *in vivo* or *in vitro*. The specific PKA-dependent phosphorylation of HERGΔP1–4 was <95% compared with wild-type HERG. *In vitro* assays of mutants with single PKA sites revealed that all were targets for PKA-dependent phosphorylation (Figure 3d). The relative contribution to the total PKA-dependent phosphorylation by each was: site 1, 61 ± 4%; sites 2,3, 30 ± 3%; site 4, 6.1 ± 1%.

Whole cell patch clamp recordings from cells expressing the PKA mutants all demonstrated recognizable I_{Kr}-type current, but responses to cAMP were different from those of wild-type HERG. At baseline the voltage-activation curve for HERGΔP1–4 was left-shifted compared to wild-type HERG ($V_{\frac{1}{2}}$Δ1–4 = –15.9 ± 0.6 mV, k = 7.8). CPT-cAMP shifted the voltage-dependent activation of HERGΔP1–4 further negative ($V_{\frac{1}{2}}$ = –22.9 ± 0.25 mV, k = 9.2; Figure 2b). Current amplitude after CPT-cAMP was reduced by 9% compared to 40% seen with wild-type HERG. cAMP effects on deactivation kinetics were nearly abolished in HERGΔP1–4 (data not shown). The cAMP-mediated effects in individual site mutants were intermediate, indicating that each of the phosphorylation sites contributes to the PKA-dependent effects (Figure 3c,d).

HERG channel subunits are thought to exist in heteromultimeric complexes with one or more proteins to form cardiac I_{Kr} [6,7]. To examine the effects of cAMP on human cardiac I_{Kr} we co-expressed HERG or HERGΔ1–4 with either minK or hMiRP1. In cells expressing HERG–minK or HERG–hMiRP1, CPT-cAMP produced a leftward shift in voltage-activation and current amplitude inhibition was reduced (with hMiRP1) or absent (with minK) (Figure 2c–f). The $V_{\frac{1}{2}}$ for HERG–minK shifted from 4.0 ± 0.56 mV to –4.5 ± 1.02 mV (baseline k = 10.1, cAMP k = 15.7) after cAMP, whereas the values

Figure 2

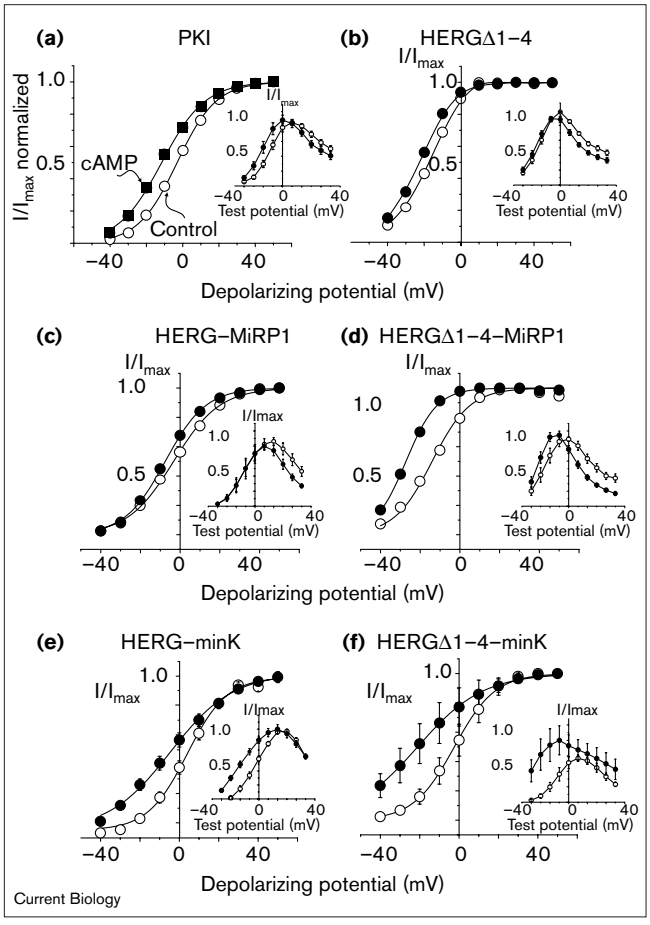

Inhibition of PKA suppresses cAMP-mediated effects on HERG and unmasks voltage activation shift. **(a)** Voltage-activation (and current–voltage (I–V) curves, insets) curves of HERG currents from cells internally dialyzed with PKI peptide before and after treatment with CPT-cAMP; means ± SEM; $n = 22$. **(b)** Normalized voltage-activation curves from HERGΔP1–4 before and after CPT-cAMP. The inset shows summary I–V curves from the same cells; means ± SEM, $n = 18$. **(c,d)** Voltage-activation and summary I–V curves for (c) HERG–hMiRP1 and (d) HERGΔ1–4–hMiRP1 before and after CPT-cAMP. **(e,f)** Voltage-activation and summary I–V curves for (e) HERG–minK and (f) HERGΔ1–4–minK before and after CPT-cAMP. White circles, control; black circles, after treatment with CPT-cAMP.

for HERG–hMiRP1 were –3.0 ± 0.4 mV to –7.5 ± 0.2 mV, respectively (baseline k = 11.7, cAMP k = 10.2). cAMP also generated a greater hyperpolarizing shift in voltage-dependent activation for HERGΔ1–4 when co-expressed with either minK (V_h = –2.4 ± 0.33 mV at baseline to –21.0 ± 0.33 mV after cAMP) or hMiRP1 (V_h = –13.7 ± 0.8 mV at baseline to –27.2 ± 0.3 mV after cAMP). Thus, when HERG is in an heteromeric complex, as in cardiac myocytes, the PKA-independent effects of cAMP on I_{Kr} appear to predominate over the PKA-mediated effects.

To investigate a possible direct cAMP–channel interaction, we performed *in vitro* binding assays of labeled cyclic

Figure 3

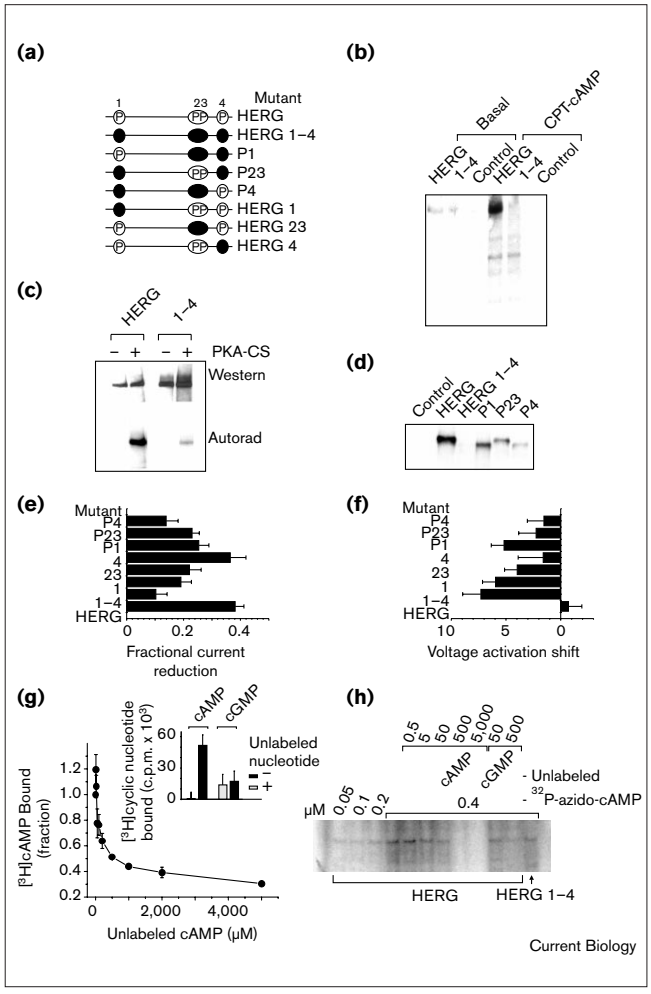

Mutation of PKA phosphorylation sites and direct cAMP-HERG binding. **(a)** Representation of the PKA-phosphorylation site mutants constructed. **(b)** *In vivo* phosphorylation of HERG, showing that wild-type HERG but not the HERGΔP1–4 mutant was ^{32}P-labeled in a cAMP-dependent fashion. **(c)** *In vitro* phosphorylation of HERG by PKA, (top) showing an anti-Myc western blot of wild-type HERG and HERGΔP1–4 and (bottom) an autoradiogram of the same blot showing >95% reduction in specific PKA-mediated phosphorylation of HERGΔP1–4. **(d)** Relative amount of *in vitro* phosphorylation of each PKA consensus site in HERG. **(e)** Summary data for cAMP-dependent current amplitude reduction for HERG and each phosphorylation site mutant. Bars represent the fractional reduction of peak tail currents after addition of CPT-cAMP (± SEM). **(f)** Data for cAMP-dependent changes in voltage-dependent activation shift for HERG and each phosphorylation site mutant. Bars represent change in voltage producing half-maximal tail current activation (V_h ± SEM). **(g)** ^{3}H-cAMP binding competition assay of immunoprecipitated HERG. Data are pooled from six determinations and normalized for comparison. Inset, binding of ^{3}H-cAMP or ^{3}H-cGMP to immunoprecipitated HERG in the absence (black bars) or presence (gray bars) of excess unlabeled cyclic nucleotide (means ± SEM; $n = 4$). **(h)** Direct photoaffinity labeling of HERG with 8-azido-[γ-^{32}P]cAMP. The signal increases in a dose-dependent fashion and is blocked by unlabeled cAMP, with complete inhibition above 200 μM. 500 μM unlabeled cGMP partially inhibits 8-azido-[γ-^{32}P]cAMP binding. HERGΔP1–4 is also labeled by 8-azido-[γ-^{32}P]cAMP.

Figure 4

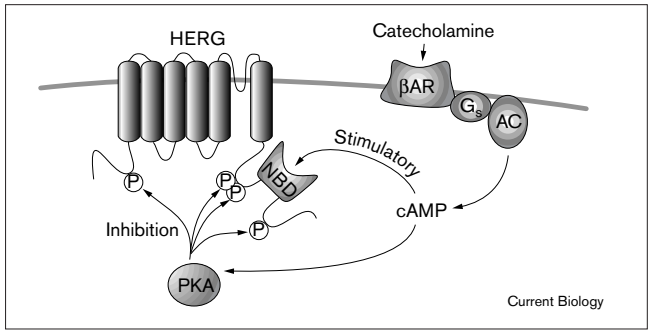

A model illustrating the complexity of cAMP regulation of HERG K^+ channel protein using two distinct pathways. Stress elevates catecholamines that stimulate β-adrenergic (βAR) receptors to activate, via G-protein (G_s), adenyl cyclase (AC). The resulting increase in cAMP produces regulation of HERG. NBD, nucleotide-binding domain.

nucleotides to the HERG protein. Immunoprecipitated HERG–Myc was used to determine direct nucleotide interaction with either 8-^{3}H-cAMP or the photo-reactive 8-azido-[γ-^{32}P]-cAMP in the presence or absence of excess unlabeled cAMP. Binding competition curves of unlabeled cAMP with ^{3}H-labeled nucleotide indicate a relatively low, but specific, affinity of the channel for cAMP (40.7 ±7.2 μM, $n = 5$ determinations; Figure 3g). The calculated specific ^{3}H-cAMP-binding capacity of HERG suggest a stoichiometry of four molecules per channel (1.3 ± 0.24 moles HERG per mole channel subunit). These results are comparable to published binding and stoichiometry data for cyclic nucleotide-gated channels (CNGC) [8,9]. Gel analysis showed specific photoaffinity labeling of HERG by 8-azido-[γ-^{32}P]cAMP that could be competitively blocked with excess unlabeled cAMP (above 100 μM; Figure 3h). Although no specific binding of cGMP was observed in either assay, excess unlabeled cGMP could partially inhibit cAMP binding (Figure 3g, inset).

Taken together, our results show that stimuli that elevate cAMP exert multiple and complex effects on HERG function though separate signaling pathways (see model, Figure 4). PKA directly phosphorylates HERG, producing an inhibition of current at all voltages, accelerated deactivation and a rightward shift in voltage dependence of activation. By shifting the voltage-gated activation to more depolarized potentials, PKA-dependent phosphorylation of HERG renders the channel less likely to open during action-potential voltages. PKA-dependent acceleration of deactivation kinetics would reduce the unique control HERG/I_{Kr} has on the rapid repolarizing phase of the cardiac myocyte action potential. Thus, the PKA-dependent effects combine to decrease effective HERG/I_{Kr} activity. Simultaneously, cAMP directly binds to the HERG protein and shifts the voltage-dependence of activation to depolarized potentials. Although this direct effect counterbalances the PKA-dependent shift in voltage activation, the current inhibition and accelerated deactivation remain unopposed, and the net effect is diminution of HERG current. When HERG is complexed with minK or MiRP, however, the relative contribution of direct cAMP effects on I_{Kr} is accentuated.

Distinct channel mutations are associated with different responses to stress and exercise. During adrenergic stimulation in individuals with LQT1, the main cAMP-responsive repolarizing current, I_{Ks}, is reduced or absent. Our data suggest that, for LQT1, stress-induced cAMP may also reduce the only remaining delayed rectifier current, I_{Kr}, thus further impairing repolarization. Our results correlate well with clinical data and provide a mechanistic link in the pathophysiology of stress-induced arrhythmia in LQTS. If the PKA-dependent pathway could be selectively inhibited while cAMP was still allowed to rise, then adrenergic stimulation might have a beneficial effect on myocyte membrane repolarization. Thus, this demonstration of cAMP's dual pathways of HERG regulation may provide a basis for a more genotype-specific therapy.

Supplementary material

Supplementary material including additional discussion and methodological details is available at http://current-biology.com/supmat/supmatin.htm.

Acknowledgements

We thank Charles Rubin and David Clapham for helpful discussion and Zhihui Yu for technical assistant with construction of HERG mutants. Thanks to Steve Goldstein for the generous gift of the hMiRP1 cDNA. G.I.F. is an Established Investigator of the American Heart Association. This work was supported in part by grants from the Council for Tobacco Research, Inc. (G.I.F.), American Heart Association (T.V.M.) and the N.I.H. (T.V.M.).

References

1. Roden DM, Lazzara R, Rosen M, Schwartz PJ, Towbin J, Vincent GM: **Multiple mechanisms in the Long-QT syndrome: current knowledge, gaps, and future directions.** *Circulation* 1996, **94:**1996-2012.
2. Curran ME, Splawski I, Timothy KW, Vincent GM, Green ED, Keating MT: **A molecular basis for cardiac arrhythmia: *HERG* mutations cause long QT syndrome.** *Cell* 1995, **80**:795-803.
3. Sanguinetti MC, Jurkiewicz NK, Scott A, Siegl PK: **Isoproterenol antagonizes prolongation of refractory period by class III antiarrhythmic agent E-4031 in guinea pig myocytes.** *Circ Res* 1991, **69:**77-84.
4. Palma E, Yu Z, Fishman GI, McDonald TV: **Cyclic AMP-dependent phosphorylation and regulation of HERG.** *Circulation* 1998, **98(suppl I):**57.
5. Thomas D, Zhang W, Karle CA, Kathöfer S, Schöls W, Kübler W, Kiehn J: **Deletion of protein kinase A phosphorylation sites in the HERG potassium channel inhibits activation shift by protein kinase A.** *J Biol Chem* 1999, **274:**27457-27462.
6. McDonald TV, Yu Z, Ming Z, Palma E, Meyers MB, Wang KW, *et al.*: **A minK-HERG complex regulates the cardiac potassium current I_{Kr}.** *Nature* 1997, **388**:289-292.
7. Abbott GW, Sesti F, Splawski I, Buck ME, Lehmann MH, Timothy KW, *et al.*: **MiRP1 forms I_{Kr} potassium channels with HERG and is associated with cardiac arrhythmia.** *Cell* 1999, **97:**175-187.
8. Goulding EH, Tibbs GR, Siegelbaum SA: **Molecular mechanism of cyclic-nucleotide-gated channel activation.** *Nature* 1994, **372:**369-374.
9. Zagotta WN, Siegelbaum SA: **Structure and function of cyclic nucleotide-gated channels.** *Annu Rev Neurosci* 1996, **19:**235-263.